Available online at www.sciencedirect.com

ScienceDirect

Scripta Materialia 99 (2015) 93–96

Scripta MATERIALIA

www.elsevier.com/locate/scriptamat

The use of high-entropy alloys in additive manufacturing

Yevgeni Brif, Meurig Thomas and Iain Todd*

Department of Materials Science and Engineering, University of Sheffield, Mappin Street, Sheffield S1 3JD, UK

Received 3 November 2014; revised 26 November 2014; accepted 30 November 2014
Available online 17 December 2014

An equiatomic FeCoCrNi high-entropy alloy is used as an input material for selective laser melting. The material is characterized using X-ray diffraction, scanning electron microscopy, thermal analysis and mechanical testing to investigate the feasibility of using high-entropy alloys in additive manufacturing and the resulting tensile properties. Results show that not only does the alloy preserve its single-phase solid-solution state, but it also exhibits high strength and ductility that are comparable to engineering materials like stainless steels.

Keywords: High-entropy alloys; Laser deposition; Tension test; XRD

Since high-entropy alloys (HEAs) were first reported 10 years ago [1,2], they have attracted significant attention from researchers globally [3,4]. As the potential for major developments using conventional alloy design is decreasing, HEAs show considerable promise from both a scientific and an application perspective. The generally accepted definition of an HEA is that it is a system of five or more principal elements, each having a concentration between 5 and 35 at.%. As a result of the multi-component nature of HEA systems, they are expected to exhibit a complex microstructure with various phases and intermetallics. This is not always the case, however; the microstructure of HEAs is a simple, single-phase solid solution, and, although the majority of current research is focused on equimolar systems containing five or more principal elements, the characteristic high-entropy microstructure has also been reported for both non-equimolar systems [5] and for four-component alloys [6,7].

The underlying mechanism behind the HEAs is a minimization of the Gibbs free energy through a balance between entropy and enthalpy [8]. The vast number of possible alloy combinations and the possibility of tailoring the constituent elements to tune the final properties of the HEA are the two major reasons for the increasing scientific attention in this field. Despite the growing interest in HEAs, most published works focus mainly on the thermodynamic aspects of HEAs and the resulting microstructure. Although data pertaining to the mechanical properties of HEAs are available in the literature, at present it is largely limited to monotonic compressive loading and bulk hardness testing [9–11].

Recently, the tensile properties of various HEA systems have been reported, indicating that they are extremely ductile and can be work hardened [5,7,12,13]. With the exception of the work of Kunce et al. [14] and works involving HEA coatings prepared by laser cladding [15,16], all currently published works utilized arc melting or an induction furnace followed by casting to produce the high-entropy alloys: these methods are unlikely to present an industrially suitable route for the production and use of HEAs. As these alloys are relatively complex systems, it is safe to assume that their implementation will be limited to highly demanding applications, where the potential benefit of HEAs will overcome the inherent complexity and high levels of control required to produce them. With this in mind, it would appear that additive manufacturing (AM), which facilitates a high level of local process control and generates rapid solidification cooling rates, may be a suitable candidate for utilizing HEAs as an engineering material. This research was conducted with two major aims: to demonstrate the feasibility of producing HEAs via an AM route and yo report the mechanical properties of a four-component FeCoCrNi HEA produced by AM.

In order to address the first research aim, selective laser melting (SLM) was chosen as the AM method in this research. SLM is one of the most popular and widespread of the AM methods. As such, it is a good starting point for exploring these new alloys.

The AM specimens were manufactured from pre-alloyed, gas-atomized FeCoCrNi powder, the chemical composition of which is provided in Table 1. All specimens were manufactured using a Renishaw SLM125 machine with a maximum laser intensity of 200 W and a laser spot size of 50 μm. Two different specimen geometries were used: 10 mm cubic specimens were manufactured for thermal analysis, metallography and hardness testing, while a set of 8 mm × 8 mm × 60 mm cubic coupons were produced

* Corresponding author; e-mail: i.todd@sheffield.ac.uk

http://dx.doi.org/10.1016/j.scriptamat.2014.11.037
1359-6462/

Table 1. Chemical composition of powder, analysed using XRF (AMG Superalloys UK).

Element	Fe	Co	Cr	Ni	Al	Si	Zr	Other
wt.%	23.48	26.28	21.07	27.16	0.14	0.1	0.11	<0.05

as blanks for tensile testing. Each set of specimens were analysed (i) in the as-deposited state and (ii) after two different homogenization treatments: for 12 h at 750 and 1000 °C, followed by water quenching. To benchmark the FeCoCrNi manufactured by laser powder bed processing, a small number of 9 mm diameter cast specimens of identical composition were produced using an Edmund Buhler MAM-1 electric arc melter with a water-cooled copper mould.

The effect of processing parameters on the microstructure and properties is emphasized in powder-bed AM technologies, as the fusion between the deposited powder layers depends on the melt penetration depth of the laser beam. If the powder bed layer thickness is greater than the depth of the melt pool, the layer will not be completely melted and only partial inter-layer bonding will be achieved. In the absence of a robust process parameter set for selective laser melting of FeCoCrNi powder, we employed a numerical approach based on the Rosenthal model [17] (see e.g. Eq. (1) in Ref. [18]) to provide an initial prediction for the melt penetration depth as a function of laser beam power, q (W), and velocity, v (m s^{-1}). For the purpose of these preliminary calculations, the laser beam power was fixed at the maximum available for the Renishaw SLM125 platform of $q = 200$ W and, based on previous analysis by Deffley [19], the fraction of absorbed beam power was estimated to be 0.25. The powder bed substrate was fixed at room temperature and the beam velocity was set to $v = 0.3$ m s^{-1}.

In order to accurately simulate the melt pool geometry using the Rosenthal model, the material thermal properties are required. As physical property data are not readily available for this alloy, the thermal conductivity was assumed to lie in the range $80<k<100$ W m^{-1} K^{-1}, which is within the thermal conductivity range of the constituent elements. As the measured specific heat capacity ($C_p = 444$ J kg^{-1} K^{-1} at 25 °C) for the FeCoCrNi alloy, obtained through differential scanning calorimetry (DSC) analysis, was similar to the values of the base elements, we believe this assumption to be reasonable for this work. Several numerical calculations were conducted using the Scilab software [20], in which the thermal conductivity (k) value was varied between 80 and 100 W m^{-1} K^{-1} and the melt pool depth was predicted to be in the range 45–50 μm.

On the basis of these estimated melt pool depths, two groups of specimens were manufactured. One, representing the worst-case scenario, was manufactured using a 50 μm layer thickness, right on the limit of the simulated penetration depth. The second type, representing the best-case scenario, was manufactured using a 20 μm layer thickness, which is the thinnest layer possible on the SLM device used.

Phase characterization was performed by X-ray diffraction (XRD) using a Siemens D5000 Bragg–Brentano diffractometer, with a Cu K_α radiation source ($\lambda = 1.54$ Å). Thermal stability, specific heat capacity and thermal expansion were measured using differential thermal analysis (DTA), DSC and thermomechanical analysis (TMA), respectively. DTA experiment was performed in a Perkin Elmer STA8000 machine between 40 and 1450 °C, with a heating rate of 10 °C min^{-1}. The specific heat capacity was measured using a Perkin Elmer Diamond differential scanning calorimeter between 20 and 590 °C, with a heating rate of 20 °C min^{-1}. The thermal expansion coefficient was measured using a Perkin Elmer Pyris diamond thermomechanical analyser between 25 and 500 °C, with a heating rate of 5 °C min^{-1}.

Mechanical testing was performed in accordance with ASTM E8 M at Element Materials Technology, Sheffield, UK, using round tensile bars of 20 mm gauge length and 4 mm diameter. Vickers hardness testing was performed using a Struers DuraScan automated indenter (1 kg.f load), with at least 20 measurements per sample.

Microstructural studies and chemical analysis of the SLM specimens were performed using an FEI Inspect-F scanning electron microscope equipped with an EDAX energy-dispersive X-ray spectroscopy (EDS) detector. Both as-deposited and homogenized specimens were analysed. Specimens for microstructure analysis were sectioned, mounted and prepared via a standard mechanical grinding and polishing route. The size distribution of internal porosity was measured by examining a number of 2-D planar cross-sections using light optical microscopy and employing an automated thresholding procedure in the image analysis software ImageJ.

The XRD patterns (Fig. 1) indicate that all four specimens possess a single-phase face-centred cubic (fcc) crystal structure, with $a \approx 3.58$ Å. Comparable XRD results were also obtained for specimens manufactured using beam traverse rates of 0.33, 0.36, 0.38, 0.44, 0.48 and 0.5 m s^{-1}, which indicates that a single-phase solid solution is obtainable across a range of processing parameters. DTA was used to confirm the stability of the single-phase solid solution and to obtain the melting point of this HEA. The DTA results are presented in Figure 2. It is clear from the DTA

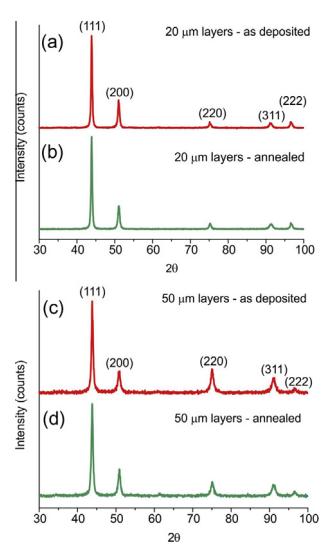

Figure 1. XRD patterns of SLM manufactured FeCoCrNi alloy: (a) 50 μm as-deposited specimen, (b) 50 μm annealed specimen, (c) 20 μm as-deposited specimen and (d) 20 μm annealed specimen.